Eur. Phys. J. D **11**, 335–339 (2000)

THE EUROPEAN PHYSICAL JOURNAL D

EDP Sciences

Kinetic energy of a trapped Fermi gas interacting with a Bose-Einstein condensate

L. Vichi[1,a], M. Amoruso[2], A. Minguzzi[2], S. Stringari[1], and M.P. Tosi[2]

[1] Istituto Nazionale per la Fisica della Materia and Dipartimento di Fisica, Università di Trento, Via Sommarive 14, 38050 Povo, Italy
[2] Istituto Nazionale per la Fisica della Materia and Classe di Scienze, Scuola Normale Superiore, Piazza dei Cavalieri 7, 56126 Pisa, Italy

Received 13 September 1999 and Received in final form 22 February 2000

Abstract. We study a confined mixture of bosons and fermions in the regime of quantal degeneracy, with particular attention to the effects of the interactions on the kinetic energy of the fermionic component. We are able to explore a wide region of system parameters by identifying two scaling variables which completely determine its state at low temperature. These are the ratio of the boson-fermion and boson-boson interaction strengths and the ratio of the radii of the two clouds. We find that the effect of the interactions can be sizeable for reasonable choices of the parameters and that its experimental study can be used to infer the sign of the boson-fermion scattering length. The interplay between interactions and thermal effects in the fermionic kinetic energy is also discussed.

PACS. 03.75.Fi Phase coherent atomic ensembles; quantum condensation phenomena –
67.40.Db Quantum statistical theory; ground state, elementary excitations –
67.40.Kh Thermodynamic properties

1 Introduction

The achievement of Bose-Einstein condensation in trapped gases [1–3] has opened new opportunities for investigating the low temperature behaviour of dilute quantum systems. Recent experimental studies have been also addressed to the search of degeneracy effects in Fermi gases [4,5] and in mixtures of bosons and fermions [6]. First experimental evidences of these effects have been recently reported in [7]. Due to the Pauli exclusion principle the effects of the interactions in a Fermi gas are much weaker than for a Bose condensate [8–13]. Therefore, the kinetic energy dominates the behaviour of the Fermi gas and is a clear indicator of its quantum degeneracy.

Interest in boson-fermion mixtures is stimulated by the fact that, whereas in a one-component spin-polarized Fermi gas the absence of interactions leads to long thermalization times which hamper the process of evaporative cooling, the collisions between the two species in a mixture can ensure fast thermalization (the so-called sympatethic cooling [14–16]). The kinetic energy of the Fermi component in such a mixture could be measured by time-of-flight techniques in an ideal experiment in which the confining potential is suddenly switched off after a fast expulsion (*i.e.* on a time scale shorter than the boson-fermion collision time) of the bosons from the trap. In this way one can avoid the effects of the interactions during the expansion of the gas. Alternatively, the kinetic energy could be obtained from inelastic photon scattering at high momentum transfer as recently shown in the case of a trapped Bose gas [17].

In this paper we analyze the behaviour of the kinetic energy of the fermionic component in a boson-fermion mixture. We find that the kinetic energy can be significantly affected by the interactions of the Fermi gas with the Bose-Einstein condensed cloud for reasonable choices of the system parameters. An important consequence of this purely quantum effect is that one can measure the sign and the strength of the boson-fermion scattering length by using the Bose component as a tunable device to change the effective potential felt by the fermions [18]. We assume a positive boson-boson scattering length, with a view to applications to mixtures of Rb–K and Na–K.

2 Interacting Fermi-Bose mixtures

For the description of the mixture at finite temperature we adopt the semiclassical three-fluid model already developed in reference [19]. We consider a system of $N_{\rm f}$ fermions of mass $m_{\rm f}$ and $N_{\rm b}$ bosons of mass $m_{\rm b}$ confined by external potentials $V_{\rm ext}^{\rm f,b}(r) = m_{\rm f,b}\omega_{\rm f,b}^2 r^2/2$ with frequencies $\omega_{\rm f}$ and $\omega_{\rm b}$. The external potentials are assumed to be spherically symmetric, the asymmetric case requiring simply

[a] e-mail: renzo@cinci.science.unitn.it
or vichi@science.unitn.it

a change of variables in the framework of the semiclassical approximation that we adopt. We include the interaction between bosons through the scattering length $a_{\rm bb}$ and the interaction between bosons and fermions through the scattering length $a_{\rm bf}$. By assuming that a single spin state is trapped for each component of the mixture, we can safely neglect the fermion-fermion interaction which is inhibited by the Pauli exclusion principle. Extensions to multi-spin configurations can be naturally made within the present formalism. In the following we will neglect the possibility of a superfluid phase for the fermionic component (for a discussion of the BCS transition in trapped Fermi gases see [20,21]) as well as the possibility of the expulsion of the bosons from the center of the cloud (this phase separation is expected to occur only for values of the coupling strengths such that the mean field contribution of the fermions is comparable with the mean field contribution of the bosons. This requires values of the parameters such that $n_{\rm f}a_{\rm bb}^3 \sim 1$. The resulting system is no more a dilute one, see [22,23]).

The spatial densities of the condensed bosons ($n_{\rm c}$), of the bosonic thermal component ($n_{\rm nc}$) and of the fermions ($n_{\rm f}$) are determined by the self-consistent solution of the following equations:

$$n_{\rm c}(r) = \frac{1}{g_{\rm bb}}\left(\mu_{\rm b} - V_{\rm ext}^{\rm b}(r) - 2g_{\rm bb}n_{\rm nc}(r) - g_{\rm bf}n_{\rm f}(r)\right), \quad (1)$$

$$n_{\rm nc}(r) = \int \frac{{\rm d}^3p}{(2\pi\hbar)^3} \times \left(\exp\left[\beta\left(\frac{p^2}{2m_{\rm b}} + V_{\rm eff}^{\rm b}(r) - \mu_{\rm b}\right)\right] - 1\right)^{-1} \quad (2)$$

and

$$n_{\rm f}(r) = \int \frac{{\rm d}^3p}{(2\pi\hbar)^3} \times \left(\exp\left[\beta\left(\frac{p^2}{2m_{\rm f}} + V_{\rm eff}^{\rm f}(r) - \mu_{\rm f}\right)\right] + 1\right)^{-1}. \quad (3)$$

Here, the effective potentials acting on the thermal boson cloud and on the fermions are given by

$$V_{\rm eff}^{\rm b}(r) = V_{\rm ext}^{\rm b}(r) + 2g_{\rm bb}n_{\rm c}(r) + 2g_{\rm bb}n_{\rm nc}(r) + g_{\rm bf}n_{\rm f}(r) \quad (4)$$

and

$$V_{\rm eff}^{\rm f}(r) = V_{\rm ext}^{\rm f}(r) + g_{\rm bf}n_{\rm c}(r) + g_{\rm bf}n_{\rm nc}(r), \quad (5)$$

where we have introduced the notations $\beta = (K_{\rm B}T)^{-1}$, $g_{\rm bb} = 4\pi\hbar^2 a_{\rm bb}/m_{\rm b}$ and $g_{\rm bf} = 2\pi\hbar^2 a_{\rm bf}/m_{\rm r}$ with $m_{\rm r}^{-1} = m_{\rm b}^{-1} + m_{\rm f}^{-1}$. The chemical potentials $\mu_{\rm b}$ and $\mu_{\rm f}$ are determined by the normalization conditions $N_{\rm b} = \int (n_{\rm c}(r) + n_{\rm nc}(r))\ {\rm d}^3r$ and $N_{\rm f} = \int n_{\rm f}(r)\,{\rm d}^3r$, which ensure the self-consistent closure of the model.

Equations (1–5) have been derived from a grand-canonical Hamiltonian in which the interactions are included in a mean-field Hartree-Fock approximation [24], by employing the semiclassical approximation for the bosonic thermal cloud and for the fermions and by taking the strong coupling limit $N_{\rm b}a_{\rm bb}/a_{\rm ho} \gg 1$ for the wavefunction of the condensate, with $a_{\rm ho} = (\hbar/m_{\rm b}\omega_{\rm b})^{1/2}$ the bosonic harmonic oscillator length. Upon averaging the Hamiltonian on the equilibrium state of the system at finite temperature we obtain the energy as the sum of various contributions: the kinetic and the external confinement energy for each of the species, as well as the boson-boson and boson-fermion interaction terms. One has

$$\begin{aligned} E &= E_{\rm kin}^{\rm f} + E_{\rm ext}^{\rm f} + E_{\rm kin}^{\rm b} + E_{\rm ext}^{\rm b} + E_{\rm int}^{\rm bb} + E_{\rm int}^{\rm bf} \\ &= \frac{3}{2}\left(\frac{m_{\rm f}}{2\pi\hbar^2}\right)^{3/2}\beta^{-5/2}\int f_{5/2}(z_{\rm f})\,{\rm d}^3r \\ &\quad + \frac{3}{2}\left(\frac{m_{\rm b}}{2\pi\hbar^2}\right)^{3/2}\beta^{-5/2}\int g_{5/2}(z_{\rm b})\,{\rm d}^3r \\ &\quad + \int V_{\rm ext}^{\rm b}(r)\left(n_{\rm c}(r) + n_{\rm nc}(r)\right)\ {\rm d}^3r \\ &\quad + \int V_{\rm ext}^{\rm f}(r)n_{\rm f}(r)\,{\rm d}^3r \\ &\quad + \frac{g_{\rm bb}}{2}\int \left(n_{\rm c}^2(r) + 2n_{\rm nc}^2(r) + 4n_{\rm c}(r)n_{\rm nc}(r)\right)\ {\rm d}^3r \\ &\quad + g_{\rm bf}\int \left(n_{\rm c}(r) + n_{\rm nc}(r)\right)n_{\rm f}(r)\,{\rm d}^3r \end{aligned} \quad (6)$$

where $f_p(z) = \Gamma(p)^{-1}\int y^{p-1}\,{\rm d}y/(z^{-1}{\rm e}^y + 1)$, $g_p(z) = \Gamma(p)^{-1}\int y^{p-1}\,{\rm d}y/(z^{-1}{\rm e}^y - 1)$ are the usual Fermi and Bose functions and $z_{\rm f,b} = \exp(\beta(\mu_{\rm f,b} - V_{\rm eff}^{\rm f,b}(r)))$. The release energy is obtained by setting the confinement potentials $V_{\rm ext}^{\rm b,f}$ in equation (6) to zero. This quantity can be measured *via* time-of-flight experiments.

At low temperature the thermal component $n_{\rm nc}$ can be safely neglected in the right hand side of equations (1, 4, 5). Similarly, when the fermionic density $n_{\rm f}$ is much smaller than the density $n_{\rm c}$ of the Bose condensate, its contribution in the right hand side of the same equations can be dropped. This is valid, for example, if the interaction strengths $g_{\rm bf}$ and $g_{\rm bb}$ have comparable size and if the trapping potential $V_{\rm ext}^{\rm f}$ is not too stiff with respect to $V_{\rm ext}^{\rm b}$. In this case the density profile of the condensate is not affected by the interaction with the fermions and the effective potential felt by the fermions takes the simplified form:

$$V_{\rm eff}^{\rm f}(r) = \begin{cases} \dfrac{1}{2}m_{\rm f}\omega_{\rm f}^2(1-\gamma)r^2 + \dfrac{g_{\rm bf}}{g_{\rm bb}}\mu_{\rm b} & \text{for } r < R_{\rm b} \\ \dfrac{1}{2}m_{\rm f}\omega_{\rm f}^2 r^2 & \text{for } r \geq R_{\rm b} \end{cases} \quad (7)$$

where

$$\gamma = \frac{g_{\rm bf}}{g_{\rm bb}}\frac{m_{\rm b}\omega_{\rm b}^2}{m_{\rm f}\omega_{\rm f}^2} \quad (8)$$

and $R_{\rm b} = (2\mu_{\rm b}/m_{\rm b}\omega_{\rm b}^2)^{1/2}$ is the radius of the condensate cloud. The potential (7) depends on temperature through

the boson chemical potential $\mu_{\rm b}$, which determines the radius $R_{\rm b}$. Full numerical calculations, including the contribution of the thermal Bose and Fermi components, show that this simplified model (hereafter called the double-parabola model) describes very well the main features of the system below the critical temperature for Bose-Einstein condensation.

In the double-parabola model, if the parameter γ in equation (8) is smaller than unity, the potential felt by the fermions has its minimum in the center of the trap. In this situation two limiting cases can be envisaged by comparing $R_{\rm b}$ with the radius of the Fermi cloud. This is approximatively given by the Fermi radius $R_{\rm F} = (2E_{\rm F}/m_{\rm f}\omega_{\rm f}^2)^{1/2}$ calculated in the absence of interactions, where $E_{\rm F} = (6N_{\rm f})^{1/3}\hbar\omega_{\rm f}$ is the Fermi energy. In the limit $R_{\rm b} \ll R_{\rm F}$ the number of bosons is much smaller than the number of fermions and thus the interactions play a minor role. Instead, in the limit $R_{\rm b} \gg R_{\rm F}$ the fermionic cloud feels a harmonic trapping potential with a renormalized frequency $\tilde{\omega}_{\rm f} = \omega_{\rm f}(1-\gamma)^{1/2}$. Finally in the case $\gamma > 1$ the repulsive interaction with the bosons is stronger than the external potential. The effective potential (7) then exhibits a local maximum at the center of the trap.

3 Scaling and role of the interactions at T = 0

Let us begin our discussion in the framework of the double-parabola model introduced in the previous section. In the case $\gamma < 1$ we can give a simple approximate solution of the model by a variational minimization of the energy functional in equation (6). At $T = 0$ this reads

$$E(T=0) = \frac{3}{5}\frac{\hbar^2}{2m_{\rm f}}(6\pi^2)^{2/3}\int n_{\rm f}^{5/3}(r)\,{\rm d}^3r + \int V_{\rm ext}^{\rm b}(r)n_{\rm c}(r)\,{\rm d}^3r + \int V_{\rm ext}^{\rm f}(r)n_{\rm f}(r)\,{\rm d}^3r + \frac{g_{\rm bb}}{2}\int n_{\rm c}^2(r)\,{\rm d}^3r + g_{\rm bf}\int n_{\rm c}(r)n_{\rm f}(r)\,{\rm d}^3r. \quad (9)$$

The variational approach (see the details in the Appendix) explicitly shows that the relevant properties of the system depend on the various parameters of the model through two adimensional combinations, which are the parameter γ in equation (8) and a parameter x given by

$$x = \sqrt{\frac{R_{\rm b}}{R_{\rm F}}} = \sqrt{\frac{m_{\rm f}\omega_{\rm f}}{2m_{\rm b}\omega_{\rm b}}}\left(\frac{15a_{\rm bb}}{a_{\rm ho}}\frac{N_{\rm b}}{(6N_{\rm f})^{5/6}}\right)^{1/5}. \quad (10)$$

At given γ, the ratio of the sizes of the two clouds in the absence of interactions determines the deviation of the kinetic energy of the Fermi component from its ideal-gas value.

We have checked numerically that the scaling in these two variables is satisfied with good accuracy also by the full numerical solution of equations (1–5) at zero temperature for any value of γ. The description of the system with only two scaling parameters instead of the eight original ones entering equations (1–3) represents a major simplification of the problem. In view of this property, in the following we shall present our discussion in terms of the scaling parameters x and γ.

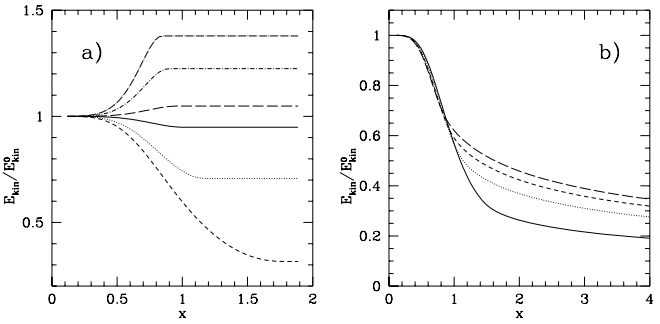

Fig. 1. Kinetic energy of the Fermi component in units of $E_{\rm kin}^0 = 3N_{\rm f}E_{\rm F}/8$ as a function of the scaling parameter x for different values of γ; (a) for $\gamma < 1$ taking the following values: $\gamma = 0.9$ (short dahses), $\gamma = 0.5$ (dots), $\gamma = 0.1$ (solid), $\gamma = -0.1$ (long dashes), $\gamma = -0.5$ (dot-short dashes) and $\gamma = -0.9$ (dot-long dashes); (b) for $\gamma > 1$ ranging from $\gamma = 1.1$ (solid curve) to $\gamma = 1.7$ (long dashed curve) in steps of 0.2.

In Figure 1a we show a plot of the kinetic energy as a function of x at zero temperature for different values of $\gamma < 1$. As x increases, the kinetic energy of the fermions goes from its non-interacting value $E_{\rm kin}^0 = 3N_{\rm f}E_{\rm F}/8$ to the strong-coupling limit $\tilde{E}_{\rm kin} = E_{\rm kin}^0(1-\gamma)^{1/2}$. As a first result of our analysis we see from Figure 1a that there is a clear correspondence, for a fixed value of x, between the value of the kinetic energy and the value of γ. Therefore the sign and the strength of the ratio between the boson-fermion and boson-boson coupling constants could be inferred from a measurement of the fermion kinetic energy.

In the case $\gamma > 1$ the fermions are expelled from the center of the trap [19,22] and form a shell around the bosons as $N_{\rm b}$ increases with respect to $N_{\rm f}$. In this case the kinetic energy of the fermions (Fig. 1b) tends to zero when $x \to \infty$.

For completeness we have also analyzed the behaviour of the mean square radius of the fermionic cloud as a function of x. For $\gamma < 1$ the asymptotic value at large x is larger (smaller) than in the ideal case for $\gamma > 0$ (< 0) (see Fig. 2a). For $\gamma > 1$ the mean square radius increases indefinitely with increasing x (Fig. 2b). These behaviours are immediately understood in terms of the behaviour of the kinetic energy shown in Figure 1.

4 The role of temperature

Let us finally examine the temperature dependence of the kinetic energy of the Fermi gas. To this purpose we have solved self-consistently the full set of equations (1–5). Of course, in the classical regime the kinetic energy is insensitive to interactions. As quantum degeneracy sets

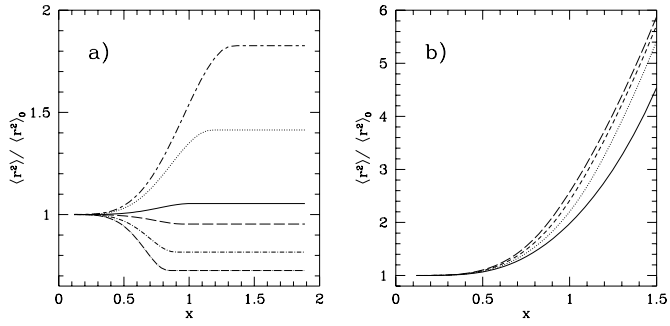

Fig. 2. Mean square radius of the Fermi component in units of $\langle r^2\rangle_0 = 3N_{\rm f}R_{\rm F}^2/8$ as a function of the scaling parameter x for different values of γ; (a) same values and notations as in Figure 1a except for the value $\gamma = 0.7$ (long dashes–short dashes) which replaces the value $\gamma = 0.9$ of Figure 1a; (b) for $\gamma > 1$, ranging from $\gamma = 1.1$ (solid curve) to $\gamma = 1.7$ (long dashed curve) in steps of 0.2.

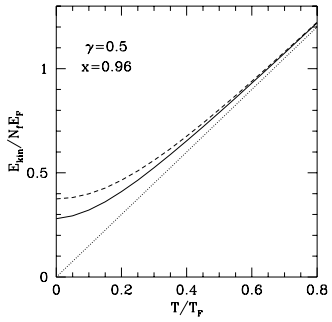

Fig. 3. Kinetic energy of the Fermi component as a function of the reduced temperature $T/T_{\rm F}$ for a choice of the scaling parameters corresponding to $m_{\rm f} = m_{\rm b} = 39$ a.u., $\omega_{\rm f} = \omega_{\rm b} = 2\pi \times 100$ s^{-1}, $N_{\rm f} = 10^4$, $N_{\rm b} = 10^6$, $a_{\rm bb} = 92a_0$ and $a_{\rm bf} = 46a_0$ where a_0 is the Bohr radius. The solid curve refers to the interacting system and the dashed line to the non-interacting one. The dotted curve shows the classical result.

in at $T < T_{\rm F}$, where $T_{\rm F} = E_{\rm F}/K_{\rm B}$ is the Fermi temperature, deviations from the classical value $3N_{\rm f}K_{\rm B}T/2$ become apparent. We show in Figure 3 the predicted behaviour for a given choice of the parameters of the mixture. The role of the interactions decreases as temperature increases. This can also be seen in Figure 4 where we plot the kinetic energy as a function of x for a choice of different temperatures.

The scaling behaviour described in Section 3 is less accurate at finite temperature. This is easily understood from the fact that the approximations leading to equation (7) become less justified as temperature increases.

5 Conclusions

We have presented a broad study of the kinetic energy of the fermionic component in a mixture of bosons and fermions in the so-called Thomas-Fermi regime

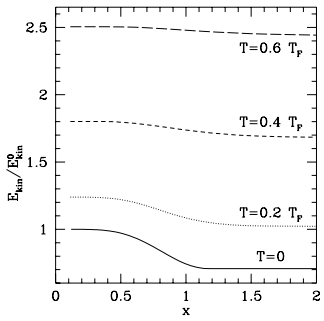

Fig. 4. Kinetic energy of the Fermi component as a function of the scaling parameter x for $\gamma = 0.5$ at different temperatures, as indicated in the figure.

($N_{\rm b}a_{\rm bb}/a_{\rm ho} \gg 1$). We have shown that at zero temperature the kinetic energy, as well as the mean square radius of the Fermi component, exhibit an important scaling behaviour in the relevant parameters γ and x defined in equations (8, 10). This has allowed us to give a systematic investigation of these physical properties on a wide range of system parameters and to understand the role of the interactions between the Fermi gas and the Bose condensate.

In particular, we have found that the shift of the fermionic kinetic energy due to the interactions becomes sizeable at appreciable values of the parameter x measuring the relative radii of the two clouds. This effect could be used to infer the sign of the boson-fermion scattering length from measurements of the fermion kinetic energy.

Finally, the role of temperature has been investigated within the self-consistent numerical solution of the full set of equations for the coupled boson-fermion mixture and the interplay between thermal and interaction effects on the kinetic energy has been demonstrated.

This work is supported by the Istituto Nazionale per la Fisica della Materia through the Advanced Research Project on BEC. One of us (L.V.) acknowledges the hospitality of the Scuola Normale Superiore di Pisa during part of this work.

Appendix A: Variational model

The scaling behaviour discussed in Section 3 can be explicitly predicted by a variational approach which turns out to be very accurate in reproducing the numerical results at $T = 0$ in the case $\gamma < 1$. The variational method is based on the minimization of the energy functional (9) within a restricted class of functions.

For $\gamma < 1$ it is convenient to describe the fermionic cloud as if it were embedded in an effective potential $V_{\rm var}(r) = m_{\rm f}\omega_{\rm var}^2 r^2/2$, where the frequency $\omega_{\rm var}$ is a variational parameter. The corresponding fermionic density profile is $n_{\rm f}(r) = 1/(6\pi^2)(2m_{\rm f}/\hbar^2)^{3/2}(E_{\rm F}^{\rm var} - m_{\rm f}\omega_{\rm var}^2 r^2/2)^{3/2}$ and the expression for the variational

energy functional takes the form

$$E_{\rm var} = E_{\rm kin} + E_{\rm ho} + E_{\rm int} = \frac{3}{8} N_{\rm f} E_{\rm F} \frac{\omega_{\rm var}}{\omega_{\rm f}} + \frac{3}{8} N_{\rm f} E_{\rm F} \frac{\omega_{\rm f}}{\omega_{\rm var}} + \frac{g_{\rm bf}}{g_{\rm bb}} \int^{\min(R_{\rm F}^{\rm var}, R_{\rm b})} \frac{1}{6\pi^2} \left(\frac{2m_{\rm f}}{\hbar^2}\right)^{3/2} \times \left(E_{\rm F}^{\rm var} - \frac{1}{2} m_{\rm f} \omega_{\rm var}^2 r^2\right)^{3/2} \left(\mu_{\rm b} - \frac{1}{2} m_{\rm b} \omega_{\rm b}^2 r^2\right) {\rm d}^3 r. \quad (A.1)$$

Here $E_{\rm F}^{\rm var} = (6N_{\rm f})^{1/3} \hbar \omega_{\rm var}$ and $R_{\rm F}^{\rm var} = (2E_{\rm F}^{\rm var}/m_{\rm f}\omega_{\rm var}^2)^{1/2}$ are the the Fermi energy and the Fermi radius calculated with the frequency $\omega_{\rm var}$. The bosons are described by the Thomas-Fermi inverted parabola $n_{\rm b}(r) = g_{\rm bb}^{-1}(\mu_{\rm b} - m_{\rm b}\omega_{\rm b}^2 r^2/2)$ with $\mu_{\rm b} = \hbar\omega_{\rm b}(15N_{\rm b}a_{\rm bb}/a_{\rm ho})^{2/5}/2$.

The integral in equation (A.1) can be carried out analytically, with the result

$$E_{\rm var}(x,\gamma,\alpha) = \frac{3}{8} N_{\rm f} E_{\rm F} \times \begin{cases} \dfrac{\alpha^2}{x^2} + \dfrac{x^2}{\alpha^2} + \gamma \dfrac{x^2}{\alpha^2} P(\alpha) & \text{for } \alpha < 1 \\ \dfrac{\alpha^2}{x^2} + \dfrac{x^2}{\alpha^2} + \gamma \dfrac{x^2}{\alpha^2} \left(-1 + \dfrac{8}{3}\alpha^2\right) & \text{for } \alpha \geq 1 \end{cases} \quad (A.2)$$

where $\alpha^2 = x^2 \omega_{\rm var}/\omega_{\rm f}$ and

$$P(\alpha) = \frac{2}{9\pi} \Big[\alpha \sqrt{1-\alpha^2}(9 - 18\alpha^2 + 40\alpha^4 - 16\alpha^6) + 3(-3 + 8\alpha^2) \arcsin(\alpha)\Big], \quad (A.3)$$

$$x = \sqrt{\frac{m_{\rm f}\omega_{\rm f}}{2m_{\rm b}\omega_{\rm b}}} \left(15 \frac{a_{\rm bb}}{a_{\rm ho}} \frac{N_{\rm b}}{(6N_{\rm f})^{5/6}}\right)^{1/5}. \quad (A.4)$$

The condition $\partial E_{\rm var}/\partial\alpha = 0$ determines the value of α and hence of $\omega_{\rm var}$. This equation has to be solved numerically, except for $\alpha \geq 1$ where the model gives the result $\omega_{\rm var} = \tilde{\omega}_{\rm f}$.

The expression (A.2) allows an explicit identification of the scaling variables introduced in Section 3. In fact, the quantity $E_{\rm var}/N_{\rm f}E_{\rm F}$ at its minimum depends only on x and γ.

Of course the variational estimate gives an upper bound for the total energy. This bound is very close to the value obtained by solving the Schrödinger equation with the potential (7). Typical deviations are less than 1% of the energy.

References

1. M.H. Anderson, J.R. Ensher, M.R. Matthews, C.E. Wieman, E.A. Cornell, Science **269**, 198 (1995).
2. K.B. Davis, M.O. Mewes, M.R. Andrews, N.J. van Drutten, D.S. Durfee, D.M. Kurn, W. Ketterle, Phys. Rev. Lett. **75**, 3969 (1995).
3. C.C. Bradley, C.A. Sackett, R.G. Hulet, Phys. Rev. Lett. **78**, 985 (1997).
4. B. DeMarco, J.L. Bohn, J.P. Burke Jr, M. Holland, D.S. Jin, Phys. Rev. Lett. **82**, 4208 (1999).
5. M. Prevedelli, F.S. Cataliotti, E.A. Cornell, J.R. Ensher, C. Fort, L. Ricci, G.M. Tino, M. Inguscio, Phys. Rev. A **59** 886 (1999).
6. M.-O. Mewes, G. Ferrari, F. Schreck, A. Sinatra, C. Salomon, Phys. Rev. A **61**, 011403 (2000).
7. B. DeMarco, D.S. Jin, Science **285**, 1703 (1999).
8. Isaac F. Silvera, Physica **109** & **110B**, 1499 (1982).
9. D.A. Butts, D.S. Rokhsar, Phys. Rev. A **55**, 4346 (1997).
10. J. Schneider, H. Wallis, Phys. Rev. A **57**, 1253 (1997).
11. G.M. Bruun, K. Burnett, Phys. Rev. A **58**, 2427 (1998).
12. H.T.C. Stoof, M. Houbiers, in Bose-Einstein Condensation in Atomic Gases, *Proceedings of the International School of Physics "Enrico Fermi"*, edited by M. Inguscio, S. Stringri, E.E. Wieman (SIF, Bologna, 1999).
13. K. Mølmer, Phys. Rev. Lett. **80**, 1804 (1998).
14. C.J. Myatt, E.A. Burt, R.W. Ghrist, E.A. Cornell, C.E. Wieman, Phys. Rev. Lett. **78**, 586 (1997).
15. E. Timmermans, R. Côté, Phys. Rev. Lett. **80**, 3419 (1998).
16. W. Geist, L. You, T.A.B. Kennedy, Phys. Rev. A **59**, 1500 (1999).
17. J. Stenger, S. Inouye, A.P. Chikkatur, D.M. Stamper-Kurn, D.E. Pritchard, W. Ketterle, Phys. Rev. Lett. **82**, 4569 (1999).
18. L. Vichi, M. Inguscio, S. Stringari, G.M. Tino, J. Phys. B: At. Mol. Opt. Phys. **31**, L899 (1998).
19. M. Amoruso, A. Minguzzi, S. Stringari, M.P. Tosi, L. Vichi, Eur. Phys. J. D **4**, 261 (1998).
20. M.A. Baranov, Yu. Kagan, M.Yu. Kagan, JETP Lett. **64**, 301 (1996).
21. H.T.C. Stoof, M. Houbiers, C.A. Sackett, R.G. Hulet, Phys. Rev. Lett. **76**, 10 (1996).
22. N. Nygaard, K. Mølmer, Phys. Rev. A **59**, 2974 (1999).
23. L. Viverit, C.J. Pethick, H. Smith, Phys. Rev. A **61**, 053605 (2000).
24. S. Giorgini, L.P. Pitaevskii, S. Stringari, J. Low Temp. Phys. **109**, 309 (1997); A. Minguzzi, S. Conti, M.P. Tosi, J. Phys. Cond. Matt. **9**, L33 (1997).